



## Solar photocatalytic degradation of isoproturon over TiO<sub>2</sub>/H-MOR composite systems

Mangalampalli V. Phanikrishna Sharma, Valluri Durgakumari, Machiraju Subrahmanyam\*

*Inorganic and Physical Chemistry Division, Indian Institute of Chemical Technology, Hyderabad 500607, India*

### ARTICLE INFO

#### Article history:

Received 8 November 2007

Received in revised form 10 March 2008

Accepted 10 March 2008

Available online 20 March 2008

#### Keywords:

TiO<sub>2</sub>

H-mordenite

Zeolite

Photocatalytic degradation

Isoproturon

### ABSTRACT

The photocatalytic degradation and mineralization of isoproturon herbicide was investigated in aqueous solution containing TiO<sub>2</sub> over H-mordenite (H-MOR) photocatalysts under solar light. The catalysts are characterized by X-ray diffraction (XRD), UV–Vis diffused reflectance spectra (UV–Vis DRS), Fourier transform-infra red spectra (FT-IR) and scanning electron microscopy (SEM) techniques. The effect of TiO<sub>2</sub>, H-MOR support and different wt% of TiO<sub>2</sub> over the support on the photocatalytic degradation and influence of parameters such as TiO<sub>2</sub> loading, catalyst amount, pH and initial concentration of isoproturon on degradation are evaluated. 15 wt% TiO<sub>2</sub>/H-MOR composite is found to be optimum. The degradation reaction follows pseudo-first order kinetics and is discussed in terms of Langmuir–Hinshelwood (L–H) kinetic model. The extent of isoproturon mineralization studied with chemical oxygen demand (COD) and total organic carbon (TOC) measurements and ~80% mineralization occurred in 5 h. A plausible mechanism is proposed based on the intermediates identified by liquid chromatography–mass spectroscopy (LC–MS).

© 2008 Elsevier B.V. All rights reserved.

### 1. Introduction

Phenylurea herbicides are generally applied for weed control and among these isoproturon [3-(4-isopropylphenyl)-1,1-dimethylurea] is one of the vastly used in the world. Its solubility in water, low chemical and biochemical degradation rates results in contamination of surface [1] and ground water [2] and this in turn becomes a potential risk for environment. In this regard, different strategies have been developed for removal of these pollutants from water. Conventional biological treatment processes are very slow or ineffective and the traditional physico-chemical treatments such as adsorption on activated carbon, nano-filtration and ozonation are efficient in comparison with others but have inherent limitations in applicability, effectiveness and cost [3–5]. Hence, in recent years new processes are emerged and are commonly known as advanced oxidation processes (AOPs) [6]. The method is generally based on the generation of OH\* radicals which interact with organic pollutants leading to progressive degradation and is followed by complete mineralization. Among these heterogeneous photocatalysis with TiO<sub>2</sub>, has been considered as a promising one for the remediation of wastewater treatment [7–10]. The main drawbacks are the need for complex filtration procedures and the high turbidity that decreases the radiation flux. Such problems have motivated the development of supported photocatalysts

in which TiO<sub>2</sub> is immobilized on different adsorbent materials. In this context, zeolites have attracted greater attention due to their adsorption capacity that helps in pooling the pollutants to the vicinity of the TiO<sub>2</sub> surface and also leads to faster degradation [10,11]. Zeolites are microporous crystalline aluminosilicates with structural features that make them attractive hosts for the photochemical applications and they delocalize band gap-excited electrons of TiO<sub>2</sub> and thereby minimize the electron–hole recombination.

The objective of the present investigation is to develop an efficient TiO<sub>2</sub> supported H-mordenite (H-MOR) photocatalyst for complete mineralization of isoproturon in aqueous solution with solar light. Detailed studies on degradation kinetics, comparisons of TiO<sub>2</sub> activity with and without support are reported. An attempt also is made to identify degradation intermediates through high-pressure liquid chromatography (HPLC) and mass spectroscopy (MS). A plausible degradation mechanism is proposed for photocatalytic degradation of isoproturon. The extent of mineralization is monitored by total organic carbon (TOC) and chemical oxygen demand (COD).

### 2. Experimental

#### 2.1. Materials and methods

Isoproturon analytical grade (99.9% purity) was obtained from Rhône-Poulenc Agrochimie (France). Titanium dioxide P-25 (surface area = 50 m<sup>2</sup> g<sup>-1</sup> and particle size 27 nm) is from Degussa

\* Corresponding author. Tel.: +91 40 27193165; fax: +91 40 27160921.  
E-mail address: [subrahmanyam@iict.res.in](mailto:subrahmanyam@iict.res.in) (M. Subrahmanyam).

Corporation, Germany. Zeolite H-MOR ( $\text{SiO}_2/\text{Al}_2\text{O}_3 \approx 20$ , surface area =  $440 \text{ m}^2 \text{ g}^{-1}$ ) obtained from PQ Corporation, USA. HPLC grade acetonitrile is supplied by Ranbaxy Fine Chemicals Limited, India.  $\text{AgSO}_4$ ,  $\text{K}_2\text{Cr}_2\text{O}_7$ , and ferrous ammonium sulfate (FAS) are from S.D. Fine Chemicals Limited, India. All the solutions are prepared with de-ionized water from a Millipore device (Milli-Q). All the chemicals used in the present work are of analytical grade and used as such without further purification.

## 2.2. Preparation of $\text{TiO}_2/\text{H-MOR}$ catalysts

$\text{TiO}_2$  is dispersed on hydrogen form of mordenite zeolite surface by solid-state dispersion (SSD) method [10]. Titanium dioxide of 1, 5, 10, 15 and 20 wt% loadings over zeolite support are prepared for their photocatalytic evaluation.

## 2.3. Characterization

All the catalysts are characterized by various techniques. The X-ray diffraction (XRD) patterns of all the catalysts in this study are obtained by Siemens D-5000 X-ray diffractometer using Ni filtered  $\text{Cu K}\alpha$  radiation ( $\lambda = 1.5406$ ) from  $2\theta = 2-60^\circ$ . The Fourier transform-infra red spectra (FT-IR) are recorded on a Nicolet 740 FT-IR spectrometer (USA) using KBr self-supported pellet technique in  $4000-400 \text{ cm}^{-1}$  frequency. The UV-Vis diffused reflectance spectra (UV-Vis DRS) obtained from UV-Vis Cintra 10e spectrometer with an integrating sphere reflectance accessory using pellets of 50 mg catalyst sample ground with 2.5 g of KBr. For the scanning electron microscopy (SEM) analysis (Hitachi S-520), samples are mounted on an aluminum support using a double adhesive tape coated with gold.

## 2.4. Photocatalytic experiments

$1.14 \times 10^{-4} \text{ M}$  stock solution of isoproturon is prepared by dissolving required amount in de-ionized water. The solution is stored at  $5^\circ \text{C}$  and protected from light. This concentration is used in all the experiments unless it is stated. Appropriate amount of catalyst, 50 ml of isoproturon solution are taken in a  $100 \text{ mm} \times 50 \text{ mm}$  crystallizing dish and continuously stirred with a shaking unit before and during the irradiation experiments. Prior to the start of light experiments, dark (adsorption) experiments were carried out for 60 min under continuous stirring for better adsorption of the herbicide on to the surface of the catalyst. The initial pH of the solution is maintained by adding HCl or NaOH. The slurry solution is continuously stirred by a shaking unit at 120 rpm and illuminated under bright solar light for a required time period. Samples were withdrawn periodically from the reactor and filtered through  $0.22 \mu\text{m}$  PVDF filters (Millipore) prior to analysis. Distilled water is added at different intervals to avoid changes in concentration due to evaporation. Solar experiments are carried out between 11.00 a.m. and 3.00 p.m. in January and February, 2007 at Hyderabad.

## 2.5. Analyses

The concentration of isoproturon is monitored by Shimadzu 10AvP HPLC equipped with a variable wavelength UV detector using C-18 Phenomenex reverse phase column ( $250 \text{ mm} \times 4.6 \text{ mm}$ ). The separation was performed isocratically using a mobile phase containing a mixture of acetonitrile and water (50/50, v/v) with a flow rate of  $1 \text{ ml min}^{-1}$ . The detection was realized at 254 nm. The degradation products are analyzed by Agilent 1100 series HPLC and Agilent LC/MSD trap SL mass spectrometer equipped with an ESI source. The chromatographic separation was achieved as discussed earlier at room temperature. The mass spectrometer was operated in positive ion mode. Mass parameters adopted for ionization are

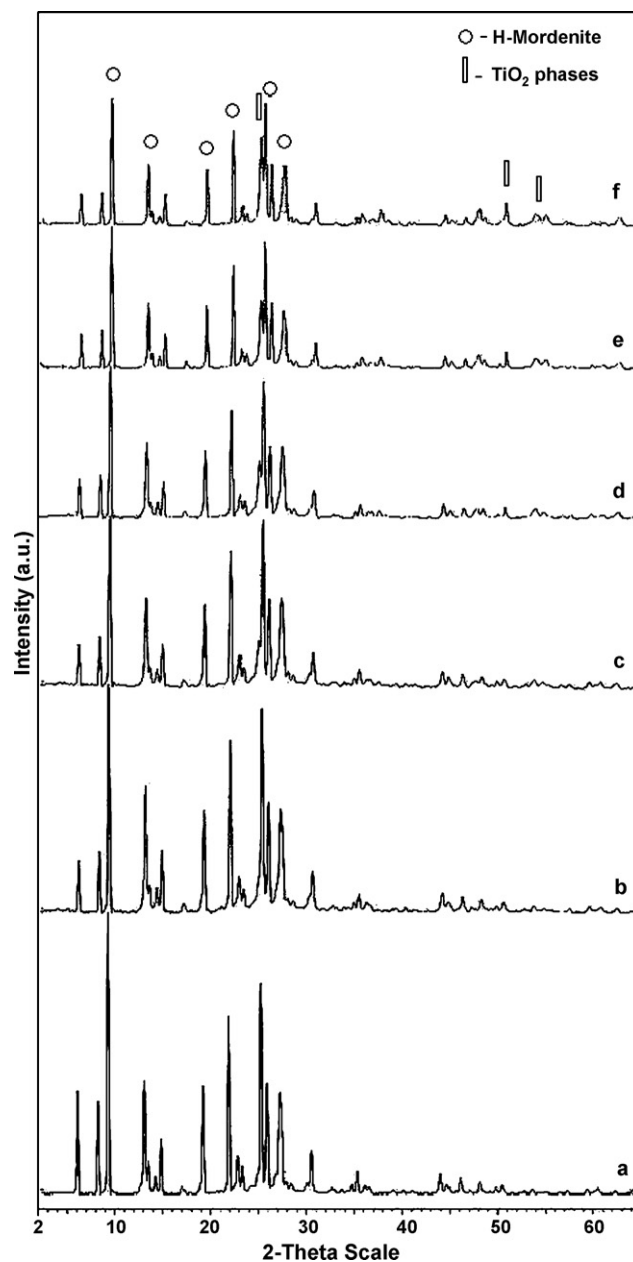


Fig. 1. XRD patterns of (a) H-MOR,  $\text{TiO}_2$  (b) 1, (c) 5, (d) 10, (e) 15 and (f) 20 wt% over H-MOR.

capillary voltage at 4 kV, capillary temperature at  $325^\circ \text{C}$ , nebuliser gas and dry gas (nitrogen) pressure at 30 psi and  $8 \text{ l min}^{-1}$ , respectively. Helium was used as collision gas at a pressure of 60 psi and collision energies used were 1–20 eV throughout the work. The extent of mineralization is analyzed through the reduction in TOC value using Shimadzu TOC-VCPN analyzer and COD analysis by titrimetric method (5520C) with dichromate solution as the oxidant in strong acid media [12].

## 3. Results and discussion

### 3.1. Characterization

The XRD pattern of H-MOR support and  $\text{TiO}_2$  loadings on the support are shown in Fig. 1. The H-MOR used for the preparation of catalysts matches with JCPDS (80-0643) database ( $d = 9.1, 3.45, 3.97$  and  $3.21 \text{ \AA}$ ) and thus confirm the mordenite phase. The  $\text{TiO}_2$

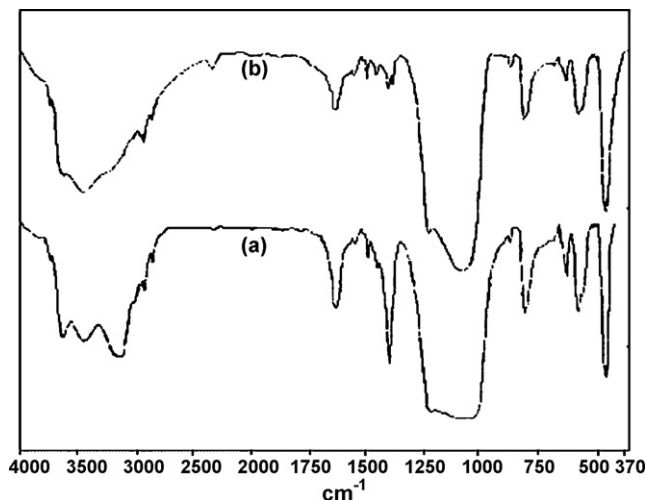


Fig. 2. FT-IR spectra of (a) H-MOR and (b) 15 wt% TiO<sub>2</sub>/H-MOR.

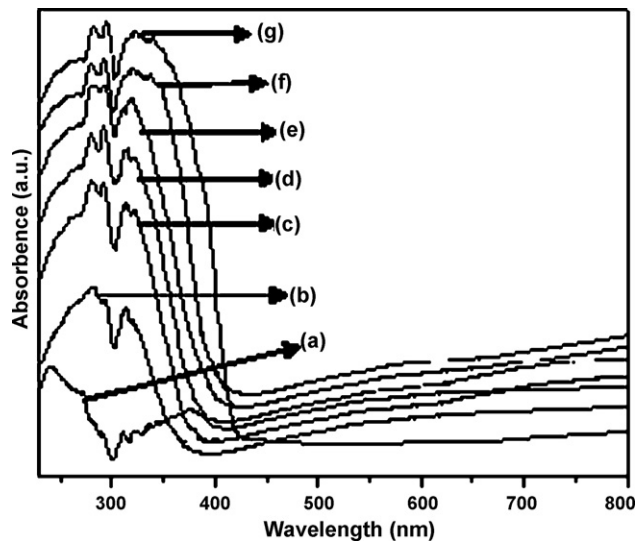


Fig. 3. UV-Vis DRS spectra of (a) H-MOR and TiO<sub>2</sub> (b) 1 wt%, (c) 5 wt%, (d) 10 wt%, (e) 15 wt%, (f) 20 wt% over H-MOR and (g) TiO<sub>2</sub>.

dispersed on H-MOR catalysts are showing that zeolite structure is intact even after dispersion. The presence of TiO<sub>2</sub> over the support is appearing from 5 wt% and above loadings, but not at lower loadings. This is because TiO<sub>2</sub> at low content is having high dispersion. The TiO<sub>2</sub> supported samples results a decrease in the intensity of characteristic peaks of H-MOR with an increasing trend of characteristic peaks of TiO<sub>2</sub> ( $d = 3.5, 1.89, 1.69$  and  $1.66 \text{ \AA}$ ) with loading. The XRD data confirms the presence of TiO<sub>2</sub> and structure of mordenite is unaffected in the prepared catalysts.

The infrared spectra of H-MOR and TiO<sub>2</sub> supported over H-MOR are shown in Fig. 2. In H-MOR alone peaks from 3150 to 3630 cm<sup>-1</sup> corresponds to O–H stretching frequencies of surface hydroxyls and physisorbed water molecules. The peak at 1630 cm<sup>-1</sup> corresponds to Lewis acidity given by Si/Al in H-MOR and the peak corresponds to 1400 cm<sup>-1</sup> is Bronsted acidity reflecting physisorbed OH presence on the surface. The framework vibration bands at 1050–1250, 750–820 and 500–650 cm<sup>-1</sup> are structure sensitive and they belong to asymmetric-stretch, symmetric-stretch and double ring vibrations, respectively [13]. The stretching frequencies between 500 and 1200 cm<sup>-1</sup> are assigned to tetrahedron (TO<sub>4</sub>) framework vibrations. The vibration bands are around 1232 and 1081 cm<sup>-1</sup> which are attributed to the asymmetric stretching of tetrahedron–oxygen–tetrahedron (T–O–T) groups. The symmetric stretching modes of T–O–T groups are observed around 800 and 544 cm<sup>-1</sup> and the band at 460 cm<sup>-1</sup> is due to the bending mode of T–O–T. When TiO<sub>2</sub> is added to H-MOR by SSD method, it may disperse well on the surface of zeolite framework and hence the possibility of displacement of physisorbed OH on the surface of the support. This may be the reason for decreasing intensity of the bands 3150–3630, 1400, and 1220–1080 cm<sup>-1</sup>. Thus, it may be concluded that TiO<sub>2</sub> is well dispersed on the support without interacting H-MOR framework.

The UV-Vis diffused reflectance spectra of TiO<sub>2</sub>/H-MOR are shown in Fig. 3. These are examined to understand the size quantization effect and the TiO<sub>2</sub> interaction with the zeolite. The position of the absorption edge for anatase is around 380 nm (band gap energy 3.2 eV), it is blue-shifted (30–40 nm) at lower loadings of TiO<sub>2</sub> and the shift is decreased with increasing loadings. This may be due to the highly dispersed and small size of anatase crystal in titania [10,14]. The UV-Vis DRS results may confirm the absence of Ti–O–Si linkage in these systems.

The surface morphology of H-MOR and 15 wt% TiO<sub>2</sub>/H-MOR are investigated by SEM and the micrographs are presented in Fig. 4. The surface morphology of H-MOR zeolite shows spherical

like crystals which are in the micron range ( $<1 \mu\text{m}$ ), and there is no considerable change in morphology of TiO<sub>2</sub> supported zeolite. The photograph of TiO<sub>2</sub> loaded zeolite is exhibiting well-dispersed white crystals of TiO<sub>2</sub> on the surface of zeolite.

### 3.2. Photocatalytic activity

#### 3.2.1. Adsorption studies

Prior to photocatalytic experiments adsorption and photolysis studies are carried out. The isoproton solution was kept in dark without catalyst for 10 days and no degradation is observed. Fifty milligrams of the catalyst in 50 ml of isoproton ( $1.14 \times 10^{-4} \text{ M}$ ) solution is allowed under stirring in dark. Aliquots were withdrawn at regular intervals and the change in isoproton concentration is monitored by HPLC. The extent of equilibrium adsorption was determined from the decrease in isoproton concentration. Maximum adsorption is reached within 60 min for H-MOR (25%) and TiO<sub>2</sub>/H-MOR systems (15–20%) and no significant concentration decrease even after 24 h. This illustrates the establishment of adsorption equilibrium as 60 min and is chosen as the optimum equilibrium time for all the future experiments. The photolysis (without catalyst) experiment is carried out under the solar light by taking 50 ml of isoproton solution in glass reactor and the results are depicted in Fig. 5 and only 2–4% of degradation is observed after 10 h of solar irradiation. There is no significant degradation over H-MOR zeolite and this illustrates that there is no photocatalytic ability for H-MOR and it acts only as a support.

#### 3.2.2. Determination of TiO<sub>2</sub> loading over H-MOR

The effect of TiO<sub>2</sub> loading on H-MOR zeolite is investigated with 1–20 wt% content and the results are depicted in Fig. 5. All the studies are carried out by at 1 g l<sup>-1</sup> catalyst amount in  $1.14 \times 10^{-4} \text{ M}$  isoproton solution. The degradation rate of isoproton increases with increasing TiO<sub>2</sub> loading from 1–15 wt% and at above loadings it is decreased. The 15 wt% TiO<sub>2</sub> loading covering in a monolayer surface over H-MOR showed efficient degradation rate and complete disappearance of isoproton as it is observed within 60 min. At higher loadings of titania over zeolite framework a loss in activity may be attributed to

- The shielding of incident light by TiO<sub>2</sub> particles.
- Decreased adsorption capacity of H-MOR as titania is blocking the pores.

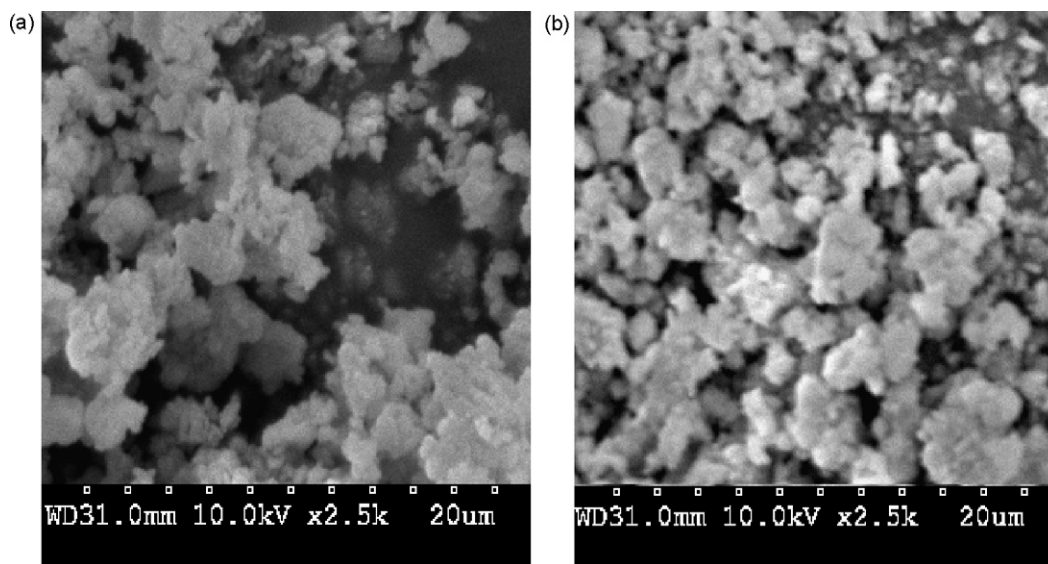


Fig. 4. SEM photographs of (a) H-MOR and (b) 15 wt% TiO<sub>2</sub>/H-MOR.

- Some TiO<sub>2</sub> particles may not be close to zeolite surface and there is a possibility of faster electron-hole recombination resulting low degradation rates.

In view of the above, the TiO<sub>2</sub> loading over the support needs to be optimized simultaneously retaining the active sites for adsorption in order to achieve the effective synergism.

### 3.2.3. Effect of isoproturon concentration

The effect of pollutant concentration is an important parameter in wastewater treatment. The isoproturon  $7.28 \times 10^{-5}$ ,  $1.14 \times 10^{-4}$  and  $2.42 \times 10^{-4}$  M concentrations are investigated over 15 wt% TiO<sub>2</sub>/H-MOR at  $1 \text{ g l}^{-1}$  catalyst amount and the results are depicted in Fig. 6. It is observed that there is a slight difference in degradation rate at  $7.28 \times 10^{-5}$  and  $1.14 \times 10^{-4}$  M concentrations compared to  $2.42 \times 10^{-4}$  M. This may be the insufficient OH radical availability for isoproturon molecules near the surface of catalyst at higher concentrations. It is well acknowledged that the degradation is solely depends on the OH radical generation. This infers that, there should be equilibrium between adsorption of reactant molecules and the

generation of OH radicals at the active sites of the catalyst. In the present investigation,  $1.14 \times 10^{-4}$  M solution is found to be the optimum concentration for degradation.

The influence of initial concentrations of isoproturon on the photocatalytic degradation rates are behaving pseudo-first order kinetics and the apparent rate constant for  $1.14 \times 10^{-4}$  M isoproturon solution is  $0.121 \text{ min}^{-1}$  ( $r^2 = 0.992$ ) over 15 wt% TiO<sub>2</sub>/H-MOR catalyst.

Photocatalytic oxidation of many organic substrates suggest a kinetic rate equation in the form of a modified L-H rate equation (Eq. (1)) [15–17]:

$$r = \frac{K_1 k C}{1 + K_1 C} \quad (1)$$

where 'C' is the initial concentration in  $\text{mg l}^{-1}$ , 'k' is the reaction rate constant and 'K<sub>1</sub>' is the Langmuir adsorption constant.

The experimental data has been rationalized in terms of modified L-H kinetic model to accommodate a reaction occurring at

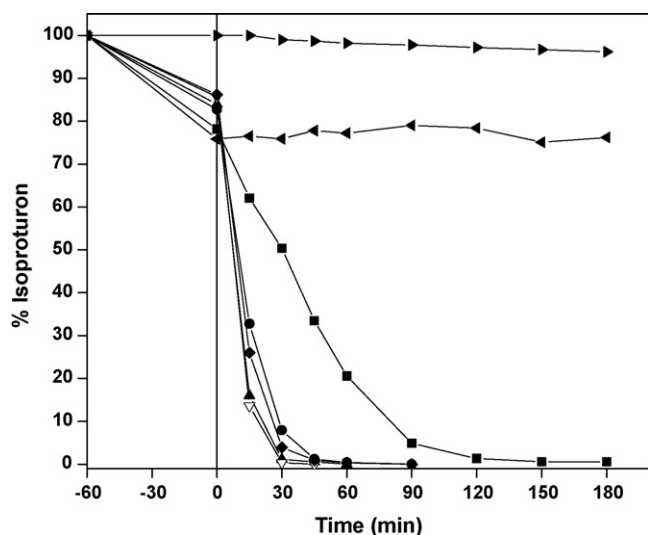


Fig. 5. Solar photocatalytic isoproturon degradation (►) photolysis, (◄) H-MOR and TiO<sub>2</sub> (■) 1 wt%, (●) 5 wt% (▲) 10 wt%, (▼) 15 wt% and (◆) 20 wt% over H-MOR.

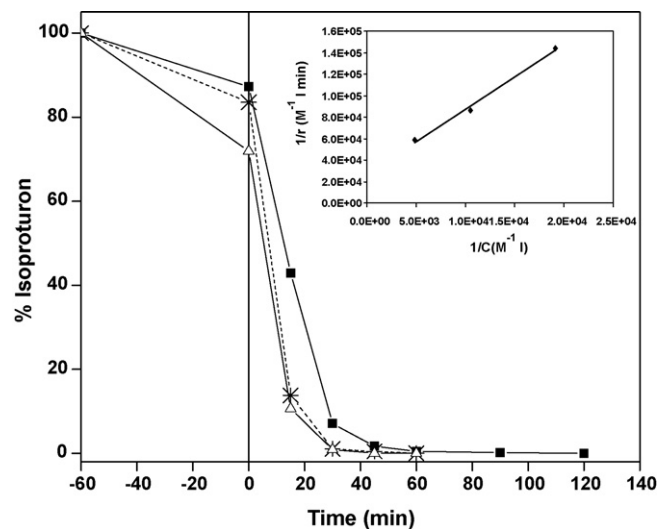


Fig. 6. (a) Effect of isoproturon concentration (■)  $2.42 \times 10^{-4}$ , (✱)  $1.14 \times 10^{-4}$  and (△)  $7.28 \times 10^{-5}$  M on the rate of degradation over 15 wt% TiO<sub>2</sub>/H-MOR and (inset) linearised reciprocal kinetic plot of the degradation of isoproturon by 15 wt% TiO<sub>2</sub>/H-MOR.



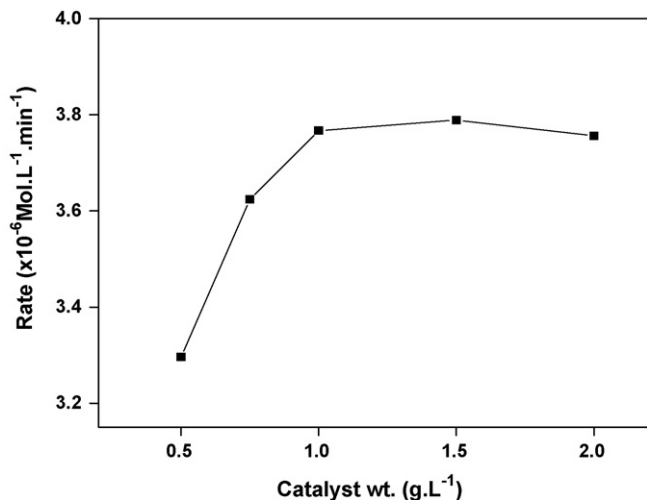


Fig. 7. Effect of 15 wt% TiO<sub>2</sub>/H-MOR catalyst amount for photocatalytic degradation of isoproturon.

solid–liquid interface (Eq. (2)).

$$\frac{1}{r} = \frac{1}{K_1 k C} + \frac{1}{k} \quad (2)$$

The rate of degradation at the surface is proportional to the surface coverage of isoproturon over the photocatalyst assuming that it is strongly adsorbed on the catalyst surface than the formed intermediates [16–18]. At lower concentrations of isoproturon, Langmuir–Hinshelwood expression has been employed as a model for kinetics of heterogeneous photocatalysis. This was confirmed by plotting the reciprocal of initial rate ( $1/r$ ) against reciprocal of initial concentration ( $1/C$ ) as is shown in inset Fig. 6. The values of  $k$  and  $K_1$  from Eq. (2) are  $3.74 \times 10^{-5} \text{ M min}^{-1}$  and  $4.41 \times 10^3 \text{ M}^{-1}$ , respectively for the degradation.

### 3.2.4. Effect of catalyst amount

To understand the optimum catalyst amount required for effective isoproturon photocatalytic degradation, 0.5, 0.75, 1.0, 1.5 and 2.0 g l<sup>-1</sup> catalyst amounts are evaluated using 15 wt% TiO<sub>2</sub>/H-MOR and the obtained results are shown in Fig. 7. By varying catalyst amounts, it is observed that 1.5 g l<sup>-1</sup> is found to be optimum. Increasing 0.5–1.5 g l<sup>-1</sup>, the rate of photocatalytic activity is increased and at higher amounts the activity is not found to be encouraging. This is due to higher amount of the catalyst makes the solution turbid resulting a control on the penetration of light into solution that inturn leads to reduction in hydroxyradical formation.

### 3.2.5. Activity comparison of TiO<sub>2</sub> and supported systems

To understand the role of support during the photocatalytic degradation of isoproturon, the amount of TiO<sub>2</sub> available over 15 wt% TiO<sub>2</sub> supported system is considered for the degradation activity and the studies are carried out using 1.5 g l<sup>-1</sup> catalyst in  $1.14 \times 10^{-4} \text{ M}$  isoproturon. From Fig. 8, it is observed that TiO<sub>2</sub> supported system is showing higher rate of degradation than TiO<sub>2</sub> alone. This is due to the higher adsorption capacity and also OH radical availability. The initial degradation is very high in supported TiO<sub>2</sub> upto 15 min and there by slow degradation rate is noted. This is perhaps due to the formation of intermediate compounds and their competitiveness for utilization of OH radicals with parent compound. The complete degradation (disappearance) of isoproturon on TiO<sub>2</sub> zeolite combinate system is observed within 45 min and over TiO<sub>2</sub> takes place in 180 min. The degradation rate on TiO<sub>2</sub> is faster upto 1 h and later decreases as discussed earlier. The mineral-

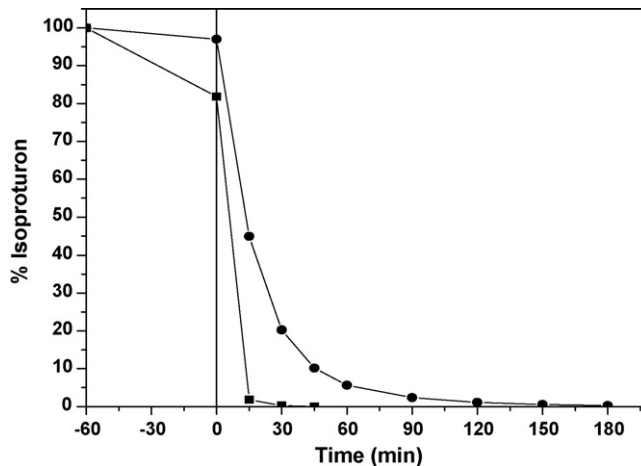


Fig. 8. Comparison of photocatalytic isoproturon degradation over (■) 15 wt% TiO<sub>2</sub>/H-MOR and (●) TiO<sub>2</sub>.

ization (TOC) reached at the time of isoproturon total disappearance over TiO<sub>2</sub>/zeolite combinate system is only about 25–30%, where as for bare TiO<sub>2</sub> it is only around 15–20%. Parra et al. also observed similar results over TiO<sub>2</sub> for isoproturon degradation [19].

The adsorption capacity of zeolite enhances the chance of OH radicals attack on the adsorbed isoproturon molecules resulting faster degradation rates. Furthermore, TiO<sub>2</sub> dispersion over H-MOR zeolite avoids particle–particle aggregation and light scattering by TiO<sub>2</sub> which provides complete harvesting of solar light. Apart from all, the delocalizing capacity of zeolite framework can effectively separate the electrons and holes produced during photo excitation of titania, thus enhancing the photocatalytic efficiency [20].

### 3.3. Recycling studies

In order to know the life and stability of 15 wt% TiO<sub>2</sub>/H-MOR catalyst recycling studies are carried out (Fig. 9). After first cycle, the oven dried catalyst is reused as such without calcination (second cycle), a slight decrease in the rate of degradation is observed compared with first cycle and it takes a little more time (60 min) for complete degradation of isoproturon. When the same catalyst is reused without calcination for third cycle, there is a slight decrease in degradation rate and it takes slightly more time compared to

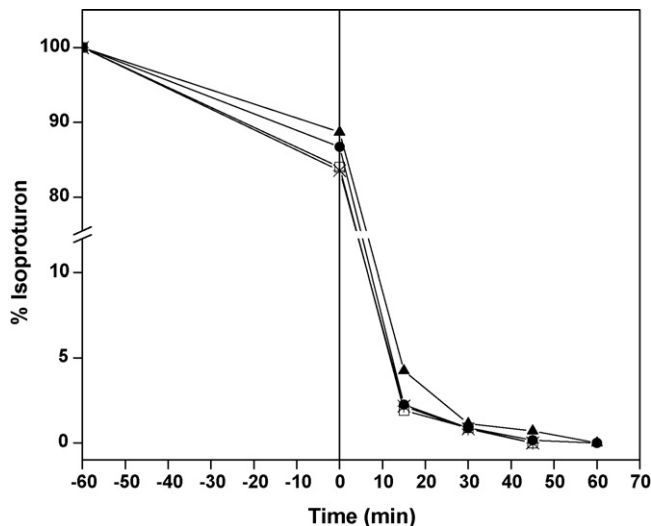
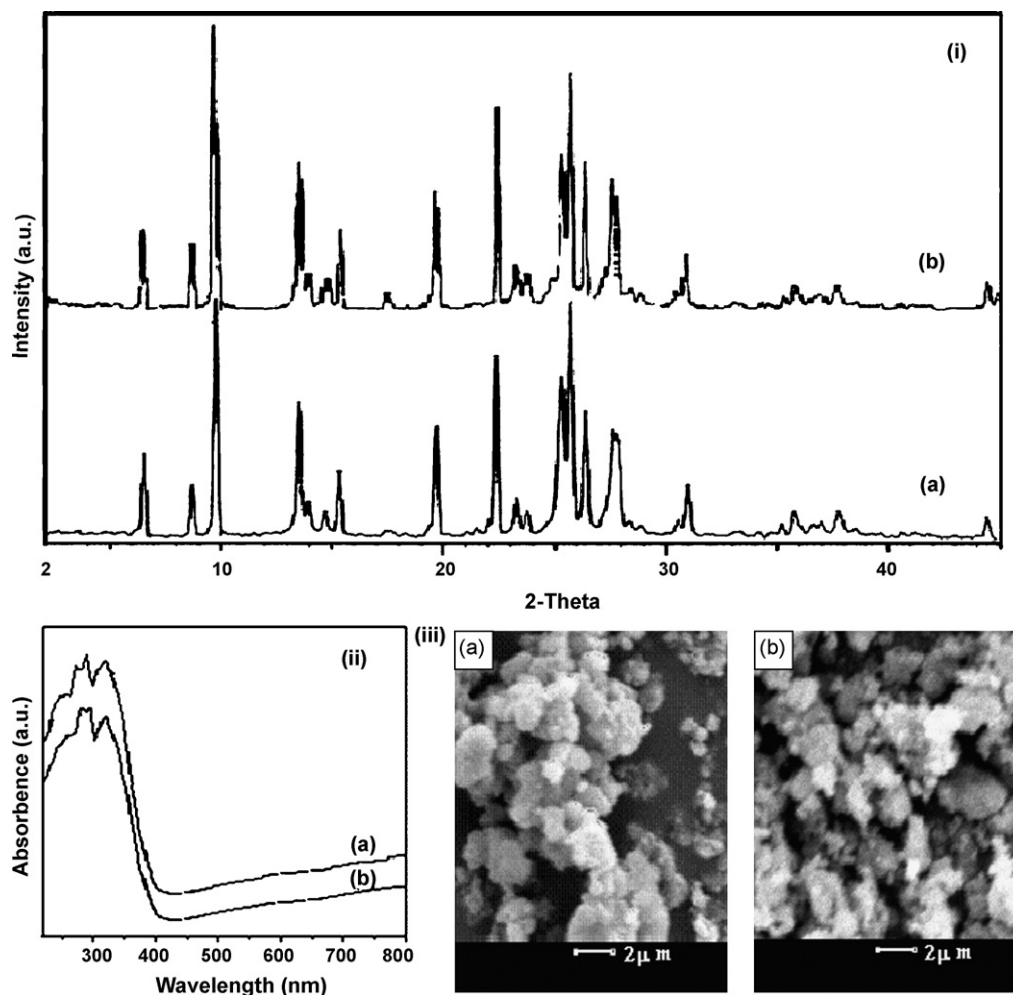


Fig. 9. Recycling activity (no. of cycles) (✱) first, (●) second, (▲) third and (□) fourth over 15 wt% TiO<sub>2</sub>/H-MOR.



**Fig. 10.** (i) XRD patterns of 15 wt% TiO<sub>2</sub>/H-MOR (a) used (after fourth cycle) (b) fresh. (ii) UV-Vis DRS spectra of 15%TiO<sub>2</sub>/H-MOR (a) used (after fourth cycle) (b) fresh. (iii) SEM photographs of 15 wt% TiO<sub>2</sub>/H-MOR (a) fresh and (b) used (after fourth cycle).

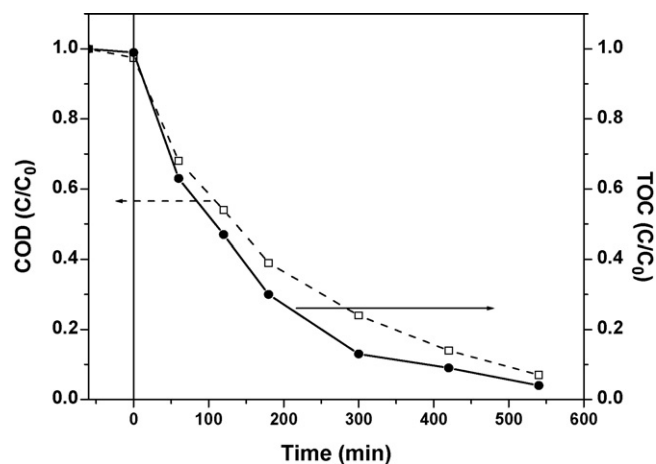
first and second cycles. The difference may be due to the accumulation of organic intermediates in the cavities and on surface of the zeolite thus affecting the adsorption in turn reducing the activity. At this stage the catalyst is calcined at 400 °C for 3 h and reused (fourth cycle), the rate of degradation is restored and is equivalent to fresh catalyst. Thus, the calcination of the used catalyst is necessary in order to maintain the activity.

Furthermore, this is substantiated by comparison of the surface characterization of fresh and used catalysts (after fourth cycle) using XRD, UV-Vis DRS and SEM techniques as depicted in Fig. 10(i-iii), respectively. The XRD pattern is well intact even after fourth cycle. The characteristic peaks of TiO<sub>2</sub> and zeolite are not changed in the fresh and used catalysts. The band gap as well as wavelength excitations are not changed in the fresh and used catalysts of the UV-Vis DRS spectra. From SEM photographs it is clear that the surface morphology do not change much and all these characteristic features illustrating that the catalyst is intact even after fourth cycle. It is proved that the catalyst is reusable for more number of cycles without losing its activity.

#### 3.4. Mineralization studies

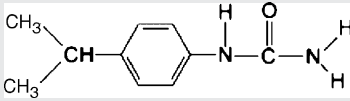
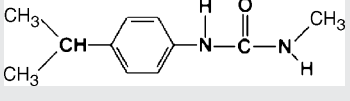
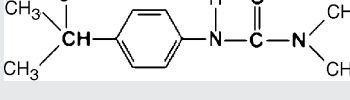
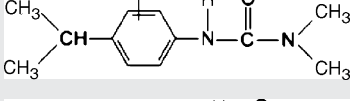
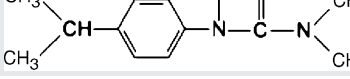
The extent of isoproturon degradation and mineralization are monitored by HPLC, COD and TOC and the results are depicted in Fig. 11. The initial TOC and COD values of isoproturon are having 16.6 and 56 mg l<sup>-1</sup>, respectively. The TOC

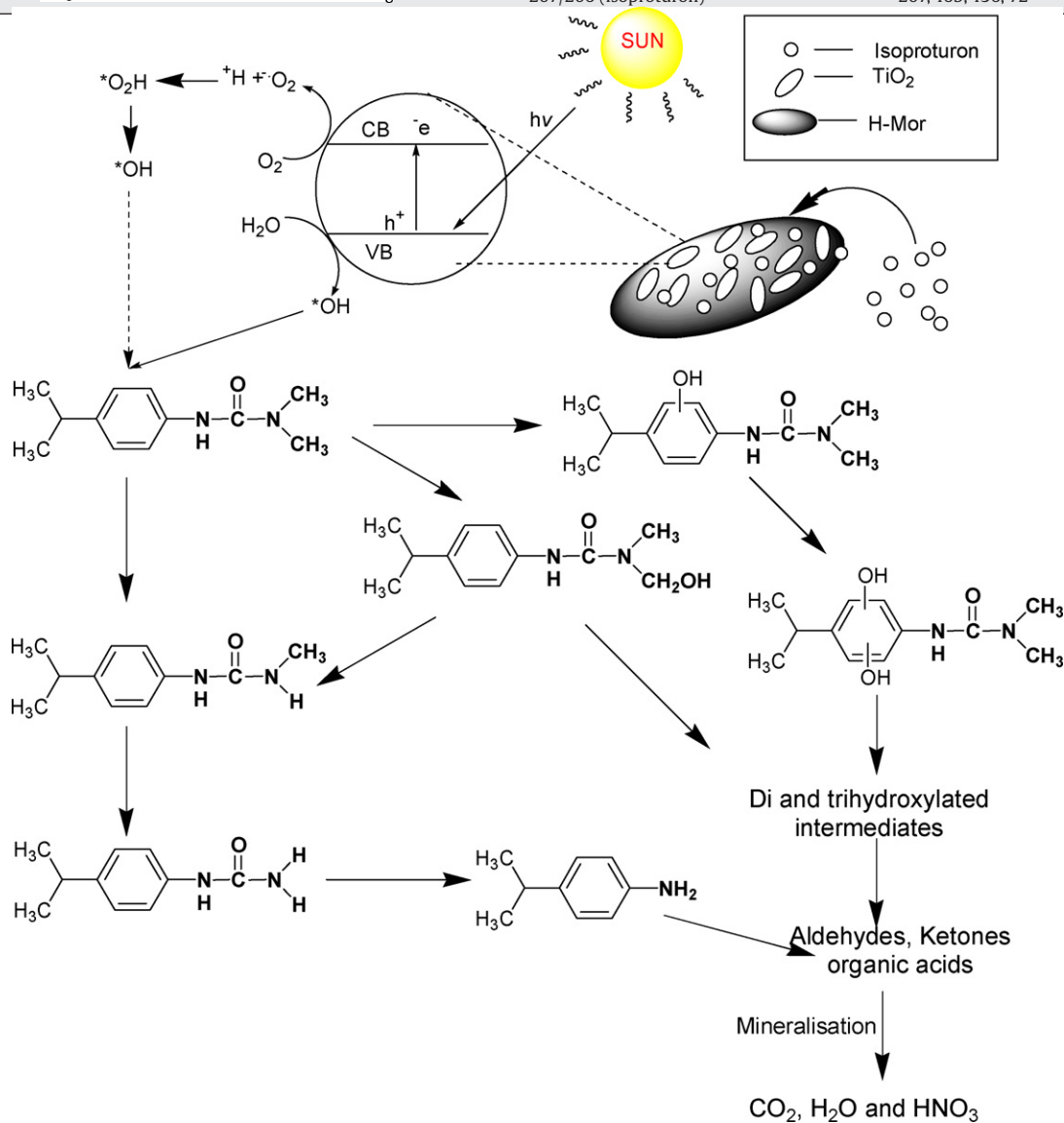
reduction is faster upto ~80% within 5 h and later it is decreased. This may be the production of more stable intermediates. The ~1 mg l<sup>-1</sup> TOC is remained at the end of the reaction, i.e., after 540 min. Also similar trend is reported by Parra et al. [21] during mineralization of phenylurea pesticides. Mineralization is faster upto 70–80% and later the degradation pattern of TOC is slow. Maletzky and Bauer [22] reported that urea is an



**Fig. 11.** Isoproturon mineralization over 15 wt% TiO<sub>2</sub>/H-MOR (□) COD and (●) TOC.

**Table 1**  
Mass spectral data for photocatalytic degradation of isoproturon as analyzed by HPLC–MS

S. no.	Compound structure	Intermediates (M+1/mol. wt.)	m/z ratios of main mass (MS) fragments
1		179/178	162, 144, 134, 119, 106, 91
2		193/192	193, 151, 136, 94
3		223/222	223, 205, 165, 134
4		223/222	223, 181, 72
5		207/206 (isoproturon)	207, 165, 136, 72



intermediate originating from degradation of nitrogen-containing organic compounds which may be the reason for slow mineralization. The left over carbon content may corresponds to aliphatic compounds, as HPLC diode array detector scans do not show any signal above 210 nm. The COD value is reduced upto ~94% at the end of reaction. Nevertheless, from the above observations a prolonged illumination brings total mineralization of the pollutant.

### 3.5. Identification of degradation intermediates and mechanism

The intermediate compounds during isoproturon degradation are identified based on LC–MS data. The data showed the formation of several intermediates and some are identified by  $m/z$  ratios of main MS fragments and is provided in Table 1. Based on the results, a plausible mechanism is proposed for photocatalytic degradation of isoproturon in Scheme 1. Some of the identified intermediates reported here were also identified and reported earlier by Amerisco et al. [23]. Isoproturon adsorbed over zeolite surface is brought to the vicinity of the  $\text{TiO}_2$ . When a photon of ultra-band gap energy ( $h\nu > E_{\text{bg}}$ ) is absorbed by  $\text{TiO}_2$  results in promotion of electrons ( $e^-$ ) from valence band (VB) to conduction band (CB), with the concomitant generation of a hole ( $h^+$ ) in the valence band. In the aqueous medium the holes react with water molecules and forms hydroxyl radicals, on the other side electrons react with oxygen molecules to form superoxide radicals and these inturn with protons ( $\text{H}^+$ ) generate another OH radical. All these OH radicals attack at different functional groups of isoproturon giving rise to several consecutive reactions. The intermediates formed by the attack of OH radicals on the aromatic ring are identified and the abstraction of hydrogen atoms of the methyl group is followed by addition of oxygen and decarboxylation lead to the formation of dealkylated intermediates. The photoreactivity also is related to the donor or withdrawing effect induced by different substituents of the aromatic ring [21]. The first hydroxylation that can occur either on the aromatic ring or on the alkyl groups leading to different monohydroxylated intermediates. Furthermore, it forms di- and poly-hydroxylated compounds and later successive oxidations lead to ketones, organic acids and ultimately lead to complete mineralization.

## 4. Conclusions

The preparation, characterization and evaluation of  $\text{TiO}_2/\text{H-MOR}$  illustrates that the adsorption property of  $\text{TiO}_2$  supported H-MOR zeolite enhances the photocatalytic degradation of isoproturon. The preparation and use of the composite system is easy and efficient for the treatment of herbicide containing wastewater. The  $\text{TiO}_2$  supported H-MOR characterization by XRD, SEM and UV–Vis DRS techniques revealed well dispersion of  $\text{TiO}_2$  on the surface of the zeolite. By increasing  $\text{TiO}_2$  loading, adsorption capacity of the zeolite is decreased due to high dispersion of  $\text{TiO}_2$  on the zeolite surface. The synergetic effect of  $\text{TiO}_2/\text{H-MOR}$  zeolite supported composite is responsible for enhanced degradation of isoproturon and its intermediates. Also, high  $\text{TiO}_2$  loading is found to be detrimental for photodegradation due to poor adsorption and distracts from utilization of holes and OH radicals. Thus, the zeolite-supported 15 wt%  $\text{TiO}_2$  composite is proven to exhibit high efficiency photocatalytic degradation of isoproturon. The catalyst amount  $1.5 \text{ g l}^{-1}$  and  $1.14 \times 10^{-4} \text{ M}$  concentration of isoproturon are found to be optimum for better degradation. The reaction is following L–H model proving that degradation is occurring at solid–liquid

interface and the reaction fits into pseudo-first order kinetics. The catalyst activity is sustainable even after fourth cycle as evidenced by XRD, SEM and UV–Vis DRS techniques.

## Acknowledgements

MVPS thank CSIR, New Delhi, India, for providing SRF grant. The authors are thankful to Dr. S. Sakunthala Madhavendra for SEM measurements.

## References

- [1] L. Nitschke, W. Schussler, Surface water pollution by herbicides from effluents of waste water treatment plants, *Chemosphere* 36 (1998) 35–41.
- [2] N.H. Spliid, B. Koppen, Occurrence of pesticides in Danish shallow ground water, *Chemosphere* 37 (1998) 1307–1316.
- [3] R.T. Meijers, E.J. Oderwaldmuller, P. Nuhn, J.C. Kruithof, Degradation of pesticides by ozonation and advanced oxidation, *Ozone-Sci. Eng.* 17 (1995) 673–686.
- [4] E. Wittmann, P. Cote, C. Medici, J. Leech, A.G. Turner, Treatment of a hard bore-hole water containing low levels of pesticide by nanofiltration, *Desalination* 119 (1998) 347–352.
- [5] P. Roche, M. Prados, Removal of pesticides by use of ozone or hydrogen peroxide/ozone, *Ozone-Sci. Eng.* 17 (1995) 657–672.
- [6] O.M. Alfano, D. Bahnmann, A.E. Cassano, R. Dillert, R. Goslich, Photocatalysis in water environments using artificial and solar light, *Catal. Today* 58 (2000) 199–230.
- [7] J.-M. Herrmann, Heterogeneous photocatalysis: fundamentals and applications to the removal of various types of aqueous pollutants, *Catal. Today* 53 (1999) 115–129.
- [8] P.R. Gogate, A.B. Pandit, A review of imperative technologies for wastewater treatment. Part I. Oxidation technologies at ambient conditions, *Adv. Environ. Res.* 8 (2004) 501–551.
- [9] M. Pratap Reddy, A. Venugopal, M. Subrahmanyam, Hydroxyapatite photocatalytic degradation of calmagite (an azo dye) in aqueous suspension, *Appl. Catal. B: Environ.* 69 (2006) 164–170.
- [10] V. Durga Kumari, M. Subrahmanyam, K.V. Subba Rao, A. Ratnamala, M. Noorjahan, K. Tanaka, An easy and efficient use of  $\text{TiO}_2$  supported HZSM-5 and  $\text{TiO}_2 + \text{HZSM-5}$  zeolite combine in the photodegradation of aqueous phenol and *p*-chlorophenol, *Appl. Catal. A: Gen.* 234 (2002) 155–165.
- [11] M.V. Shankar, S. Anandan, N. Venkatachalam, B. Arabindoo, V. Murugesan, Fine route for an efficient removal of 2,4-dichlorophenoxyacetic acid (2,4-D) by zeolite-supported  $\text{TiO}_2$ , *Chemosphere* 63 (2006) 1014–1021.
- [12] APHA, Standard Methods for the Examination of Water and Wastewater, 20th ed., American Public Health Association, American Water Works Association, Water Pollution Control Federation, Washington, DC, 1998.
- [13] P. Kovacheva, K. Arishtirova, A. Predoeva, Basic zeolite and zeolite-type catalysts for the oxidative methylation of toluene with methane, *React. Kinet. Catal. Lett.* 79 (2003) 149–155.
- [14] S. Zheng, L. Gao, Q. Zhang, W. Zhang, J. Guo, Preparation, characterization and photocatalytic properties of singly and doubly titania-modified mesoporous silicate MCM-41 by varying titanium precursors, *J. Mater. Chem.* 11 (2001) 578–583.
- [15] J.P.S. Valente, P.M. Padilha, A.O. Florentino, Studies on the adsorption and kinetics of photodegradation of a model compound for heterogeneous photocatalysis onto  $\text{TiO}_2$ , *Chemosphere* 64 (2006) 1128–1133.
- [16] A. Gora, B. Toepfer, V. Puddu, G.L. Puma, Photocatalytic oxidation of herbicides in single-component and multicomponent systems: reaction kinetics analysis, *Appl. Catal. B: Environ.* 65 (2006) 1–10.
- [17] B. Toepfer, A. Gora, G.L. Puma, Photocatalytic oxidation of multicomponent solutions of herbicides: reaction kinetics analysis with explicit photon absorption effects, *Appl. Catal. B: Environ.* 68 (2006) 171–180.
- [18] I. Poullos, I. Aetopoulou, Photocatalytic degradation of the textile dye reactive Orange 16 in the presence of  $\text{TiO}_2$  suspensions, *Environ. Technol.* 20 (1999) 479–487.
- [19] S. Parra, S. Malato, C. Pulgarin, New integrated photocatalytic-biological flow system using supported  $\text{TiO}_2$  and fixed bacteria for the mineralization of isoproturon, *Appl. Catal. B: Environ.* 36 (2002) 131–144.
- [20] A. Corma, M. Garcia, Zeolite-based photocatalysts, *Chem. Commun.* (2004) 1443–1459.
- [21] S. Parra, J. Olivero, C. Pulgarin, Relationships between physicochemical properties and photoreactivity of four biorecalcitrant phenylurea herbicides in aqueous  $\text{TiO}_2$  suspension, *Appl. Catal. B: Environ.* 36 (2002) 75–85.
- [22] P. Maletzky, R. Bauer, The photo-Fenton method—degradation of nitrogen containing organic compounds, *Chemosphere* 37 (1998) 899–909.
- [23] A. Amerisco, I. Losito, F. Palmesano, P.G. Zambonin, Photocatalytic degradation of the herbicide isoproturon: characterisation of by-products by liquid chromatography with electrospray ionisation tandem mass spectrometry, *Rapid Commun. Mass Spectrom.* 19 (2005) 1507–1516.